REPORT DOCUMENTATION PAGE

Form Approved
OMB NO. 0704-0188

1. AGENCY USE ONLY (Leave Blank)	2. REPORT DATE March 2003	3. REPORT TYPE AND DATES COVERED
		Final report 16 Au 99 - 15 mar 03

4. TITLE AND SUBTITLE
HIGH TEMPERATURE TEXTURING OF ENGINEERED
MATERIALS IN A MAGNETIC FIELD

5. FUNDING NUMBERS

6. AUTHOR(S)
Hamid Garmestani

DAAD19-99-1-0311

7. PERFORMING ORGANIZATION NAME(S) AND ADDRESS(ES)
Department of Mechanical Engineering at FAMU-FSU College of Engineering

8. PERFORMING ORGANIZATION
   FINAL REPORT

9. SPONSORING / MONITORING AGENCY NAME(S) AND ADDRESS(ES)

U. S. Army Research Office
P.O. Box 12211
Research Triangle Park, NC 27709-2211

10. SPONSORING / MONITORING
   AGENCY REPORT NUMBER

40296.2-EG-SAH

11. SUPPLEMENTARY NOTES
   The views, opinions and/or findings contained in this report are those of the author(s) and should not be construed as an official Department of the Army position, policy or decision, unless so designated by other documentation.

12 a. DISTRIBUTION / AVAILABILITY STATEMENT	12 b. DISTRIBUTION CODE
Approved for public release; distribution unlimited.	

13. ABSTRACT (Maximum 200 words)
   The primary objective of this proposal is to investigate the effect of high field/temperature in the development of texture (preferred orientation) in magnetic materials. Highly textured permanent magnet materials of $Ne_2Fe_{14}B$ have been produced using the facility constructed within the first part of the ARO support. Other materials systems including: FePd, Terfenol-D, steel and Zink material have also been processed and a highly oriented microstructure has been obtained in these materials. The success in texturing Zn-1.1%Al diamagnetic material shows that the new processing technique can also be applied to nonmagnetic materials. A new initiative in orienting nano-tube in magnetic field resulted in a huge success. These studies were carried mostly in a newly constructed high temperature furnaces funded by ARO. This facility includes two high temperature furnaces (1250^0 C and 1600^0 C) in the bore of a 20 inch resistive magnet capable of producing a uniform high magnetic field of 20 Tesla. These studies will also be carried out in the core of a 9 Tesla superconducting magnet.

14. SUBJECT TERMS		15. NUMBER OF PAGES
Texture, High temperature processing, magnetic annealing		
		16. PRICE CODE

17. SECURITY CLASSIFICATION OR REPORT	18. SECURITY CLASSIFICATION ON THIS PAGE	19. SECURITY CLASSIFICATION OF ABSTRACT	20. LIMITATION OF ABSTRACT
UNCLASSIFIED	UNCLASSIFIED	UNCLASSIFIED	UL

NSN 7540-01-280-5500

Standard Form 298 (Rev.2-89)
Prescribed by ANSI Std. 239-18
298-102

Project Description

1.0. The background:

Based on the primary goals of this proposal a 1200°C furnace was constructed within the first six months of funding. After an elaborate set of experiments and very limited success a new furnace (1600^{0}C) was constructed within the second year of funding. A number of materials systems have been tested in a variety of magnetic fields (8-20 Tesla) and temperatures (500 to 1250°C). Four materials systems have been tested (Permanent magnet $Ne_2Fe_{14}B$, Terfenol-D, Steel and Zink). These tests were continued on newer materials system including FePd and Single walled nano-tubes. This final report contains the research accomplishments and summarizes the results for these materials systems ($Ne_2Fe_{14}B$, and Zn-1.1%Al).

1.1 Theory of Magnetically Induced Grain Boundary Motion

From a phenomenological point of view, a ferromagnetic material is defined as a solid such that on a sufficiently small scale (still much larger than the lattice spacing), it has a magnetization M whose magnitude $M_s(T)$ is, to a good approximation, a function of temperature only; its direction may vary with position. The spontaneous magnetization $M_s(T)$ is attributed to exchange of forces, which tend to align neighboring electron spins parallel. Spin orbit, quadrupole, and other interactions tend to orient the aligned spin along particular crystalline axes; these interactions, in a phenomenological theory, are called forces of (magneto) crystalline anisotropy. A temperature increase causes $M_s(T)$ to decrease and finally vanishing it at the Curie temperature.

At a temperature where the spontaneous magnetization is significant and the crystalline grains are mobile along their grain boundaries, a rotation will occur to reduce the magnetic anisotropy and minimize the free energy of magnetization. In the case of powders in a viscous nonmagnetic solution such a process is very easy to observe. In a solid such a process may involve a certain amount of plasticity to satisfy compatibility. At a sufficiently high spontaneous magnetization due to a high field this may involve reorientation along magnetic domains through a process very similar to crystal plasticity.

In the following the effect of the applied field on grain boundary motion will be discussed. Note that the following discussion is not limited to ferromagnetic materials. Consider a hypothetical bicrystal of a material that has anisotropy of magnetic susceptibility (8). Let $\omega_1 < \omega_2$ be the magnetic free energies per unit volume respectively induced in the two crystals by a uniform field H. Let a small cylinder of boundary with base of *dS*

and length *dL* (Figure 1) invade the boundaries of crystal 2. Then, if ω_1 and ω_2 are independent of the boundary shape and position, the reversible change of free energy in this displacement determines the boundary pressure by $pdSdL=-(\omega_1-\omega_2)dSdL$, or $p=\omega_1-\omega_2$. This is a true pressure acting everywhere normal to the boundary.

Figure 1. A hypothetical bicrystal of arbitrary shape with free energies $\omega_1 < \omega_2$. Boundary is urged into crystal 2.
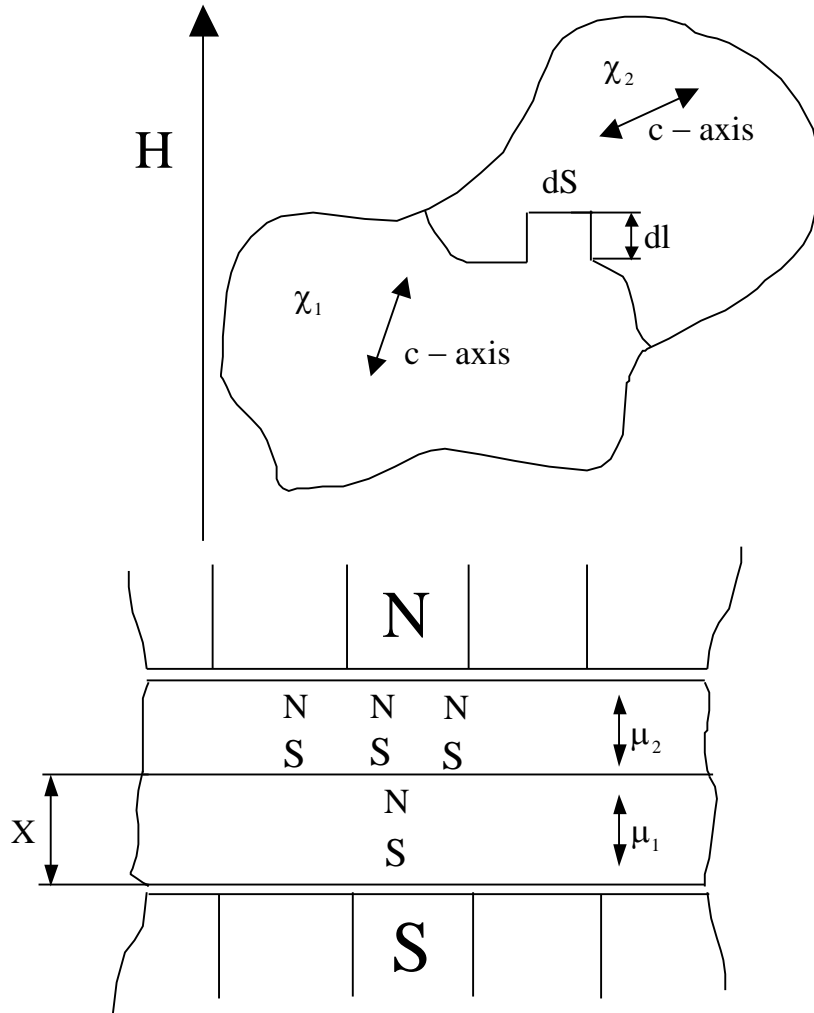

Figure 2. Diamagnetic bicrystal with $\mu_1 > \mu_2$. Field urges boundary upward.

As stated, this result is valid only if ω_1 and ω_2 are independent of the shapes and size of the crystals. The condition for this is $\chi <<1$. Then the density of magnetic free energy becomes $\omega = -\frac{1}{2}\vec{H}\chi\vec{H} = -\frac{1}{2}\chi\,H^2$, where $\chi_i = \frac{\vec{H}\chi\vec{H}}{H^2}$ is the susceptibility of crystal *i* in the direction of the

field. By substitution, one can find the pressure on the boundary of a bicrystal exposed by a uniform applied field H to be

$$p = \omega_1 - \omega_2 = \frac{\mu_o H^2}{2}(\chi_1 - \chi_2), \tag{1}$$

where χ_1 and χ_2 are the susceptibilities of crystal 1 and crystal 2, respectively, along the magnet field H. Thus, when $\chi \ll 1$, p depends only on the strength of the field and its orientation with respect to the two crystals.

If $\chi \geq 1$, the demagnetizing fields are comparable to the applied field, and the description of energies and boundary pressures becomes tractable only when the sample has a simple shape. For example, the bicrystal shown in Figure 2 has its ends and its boundary parallel to the magnetic pole pieces. The surplus of induced south poles on the boundary, arising from the discontinuity of H is given by $\mu_1 H_1 = \mu_2 H_1$ provides a simple picture of the pressure exerted by the field tending to increase the crystal of largest μ.

Let us see what form equation (1) assumes for the case of Zn. It is magnetically anisotropic and has $\chi \ll 1$. The equation (1) can be transformed to

$$p = \frac{\mu_o H^2 \Delta\chi}{2}(\cos^2\theta_1 - \cos^2\theta_2), \tag{2}$$

where θ_1 and θ_2 are the angles between the direction of the magnetic field and the c-axis in both grains of Zn bicrystals, $\Delta\chi$ is the difference of susceptibilities parallel and perpendicular to the c-axis. The force p is directed towards the grain with larger value of θ and does not depend on the sign of the magnetic field. At room temperature Zn has the following magnetic susceptibilities: $\chi_{\parallel} = -0.19 \cdot 10^{-6}$ and $\chi_{\perp} = -0.145 \cdot 10^{-6}$ (9). To estimate the possible boundary pressure for Zn, take H=32 T=32·10⁴ gauss (than can be obtained in the resistive magnet of the National High Magnetic Field Laboratory, Tallahassee, FL) and $\Delta\chi = 0.45 \cdot 10^{-7}$, then p_{max}=2300 dynes/cm²=230 J/m³. This driving force is half of that in polycrystalline bismuth at 80,000 gauss magnet field inductivity (8) and about ten times higher than in the case of Bi bicrystals (10).

2.0. Preliminary Results:

Preliminary results of the magnetic annealing on two systems of a diamagnetic material of Zn-1%Al and a Permanent Magnet materials System of NdFeB is presented in the following:

2.1 High Temperature Texturing of Ne-Fe-B

Texturing of crystalline materials under an externally applied magnetic field is an important process in many fields of materials science[1]. Heat treatment can be done at a certain temperature range in field rather than at prolonged annealing to produce a dominant crystalline orientation. A fundamental research of the effect of magnetic field on the texturing process has been initiated and applied to a number of materials systems. Here, we report on the texturing of $Ne_2Fe_{14}B$ at high temperature with an applied field.

Using a prototype furnace, a 1 x 1 cm^2 of $Ne_2Fe_{14}B$ (tetragonal structure) was annealed at 1200°C for 3 hours under argon without an applied field. X-ray diffraction (XRD) 2theta/theta scan showed a decrease in texture compared to the as-received materials.

Using a new sample with the same size, the experiment was repeated under the same conditions, except this time under a field of 8 Tesla. XRD 2theta/theta scan showed an increase in crystallinity. Figure 3 shows that the material is textured. As can be seen from the pole figure, the c-axis orientation is tilted to about 10° from the normal.

$Ne_2Fe_{14}B$ annealed without field has a random texture, whereas when annealed under an applied field a preferred orientation is produced.

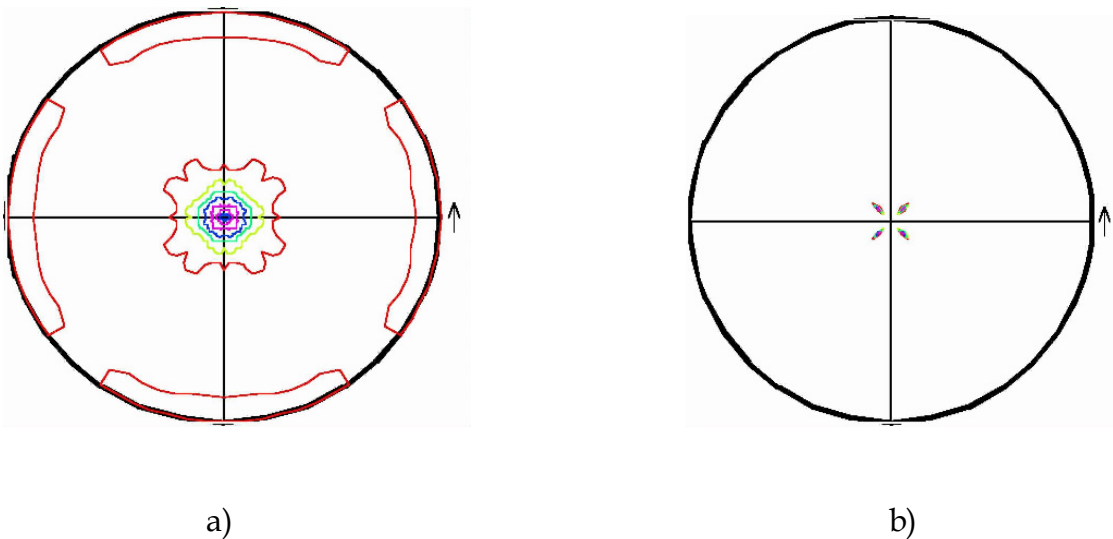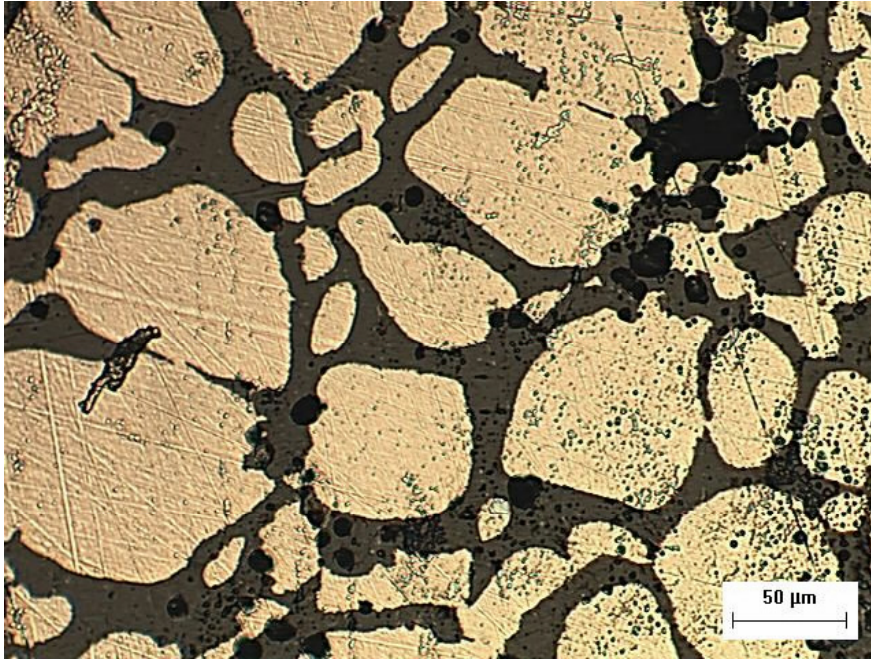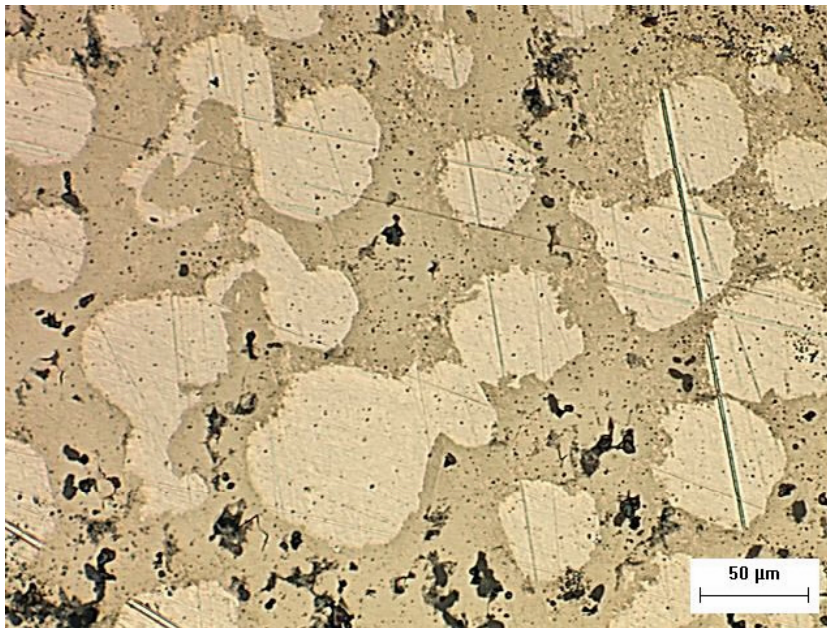a)   b)

Figure 3. Pole figures for the c-axis distribution of the a) as received materials, b) the processed materials.

a)

b)

Figure 4. Microstructure of the NdFeB samples annealed at 1200ºC. a) Without the field, b) at 15 Tesla.

2.1. Influence of High Magnetic Field on Texture Changes in Zn-1.1%Al Alloy

Introduction

It has been shown that magnetic field can affect or initiate grain boundary motion (migration) in bismuth bicrystals and coarse-grained polycrystals [1, 2]. The magnetic driving force for boundary migration is produced by the difference in diamagnetic susceptibilities of neighboring grains. In most of the anisotropic diamagnetic materials the difference in magnetic susceptibilites is significantly smaller than in bismuth. Therefore, magnetically induced boundary migration in these materials can be expected in the case of sufficiently high magnetic fields. The objective of the current study is to investigate texture changes in Zn-1.1%Al alloy during annealing under a strong magnetic field.

Experimental Procedure

Zn-1.1%Al alloy was prepared from pure metals (99.995% Zn and 99.99% Al). The casting was homogenized at 623 K for 60 hours, rolled at 573 K with the reduction of 50%, and finally rolled at 300 K with the reduction of 95%. Reduction in thickness was about 3% per pass. The direction of rolling was reversed after each pass. In order to prevent coarsening of Al-rich phase the material was stored in refrigerator at 203 K before the annealing experiments. The experiments were carried out using a resistive, steady state 32 T magnet with 32 mm bore diameter. The samples of Zn-1.1%Al alloy were annealed at the temperature of 535 K in magnetic field of 32 T. The field was applied in two different directions with respect to the rolling direction of the samples. Rolling direction (RD) coincided with magnetic strength H for one set of samples (Fig. 5(a)) and was tilted at 17±1° about the transverse direction (TD) for the other one (Fig. 5(b)). The annealing time was 20 min. Pole figures from the surface area of each sheet specimen were determined by the Schulz method using Cu K$_\square$ radiation and Philips texture goniometer. Scanning regime with amplitude of 5 mm was employed. To obtain calculated pole figures, X'Pert Texture software was used.
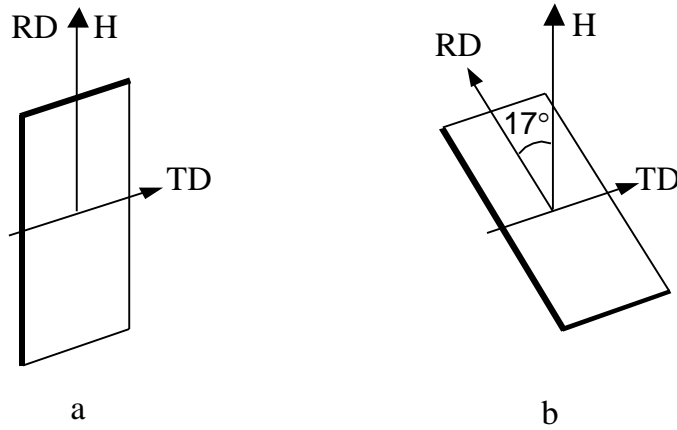
Figure 5. Orientations of specimens in respect to the field during annealing

Figure 6 shows the (0002) pole figures after rolling and after magnetic annealing. For all pole figures there are two components with c-axis tilted at 17° from normal direction (ND) to RD. Annealing with and without field results in splitting of some texture components into a few subcomponents (Figure 6 (b, c and d)). Also there is some spreading of components to ND. Annealing without magnetic field results in slight decrease in the intensity of both components (Figure 6(b)). The intensity of one component becomes smaller than the intensity of the other one. Annealing under the field parallel to the RD also decreases the intensity of both texture components (Figure 6(c)). However, in this case the difference in their intensity is bigger than after annealing without field. The intensity of one of the components increases significantly during magnetic annealing when specimen tilted at 17° with respect to the field (Figure 6(d)). The intensity of the other one remains almost the same. As seen from Figure 6 (c-d) annealing results in splitting of some texture components into a few subcomponents.

Figure 7 illustrates specimen microstructures after rolling and after magnetic annealing. The grain size in RD obtained by linear intercept method equals to 3 □m. Annealing results in the increase of grain size up to 70 □m. They remain slightly elongated in the RD with ratio of 1.4.

To comprehend the effect of magnetic annealing on texture it is necessary to consider texture alterations with and without magnetic field. Annealing without field results in the decrease of the intensity of texture components. It can be explained by the appearance of new

sharp and narrow components near ND. It seems that their appearance is due to the surface effect when the growth of grains with basal planes parallel to the surface decreases free energy of the system. Splitting and/or appearance of a large number of new components can be also a result of the decrease in statistics of grains because of significant increase of grain size. The number of grains covered by X-ray beam decreases more than 20 times. The use of scanning regime for pole figure measurements may not compensate that increase in grain size. Magnetic

a   b

c   d
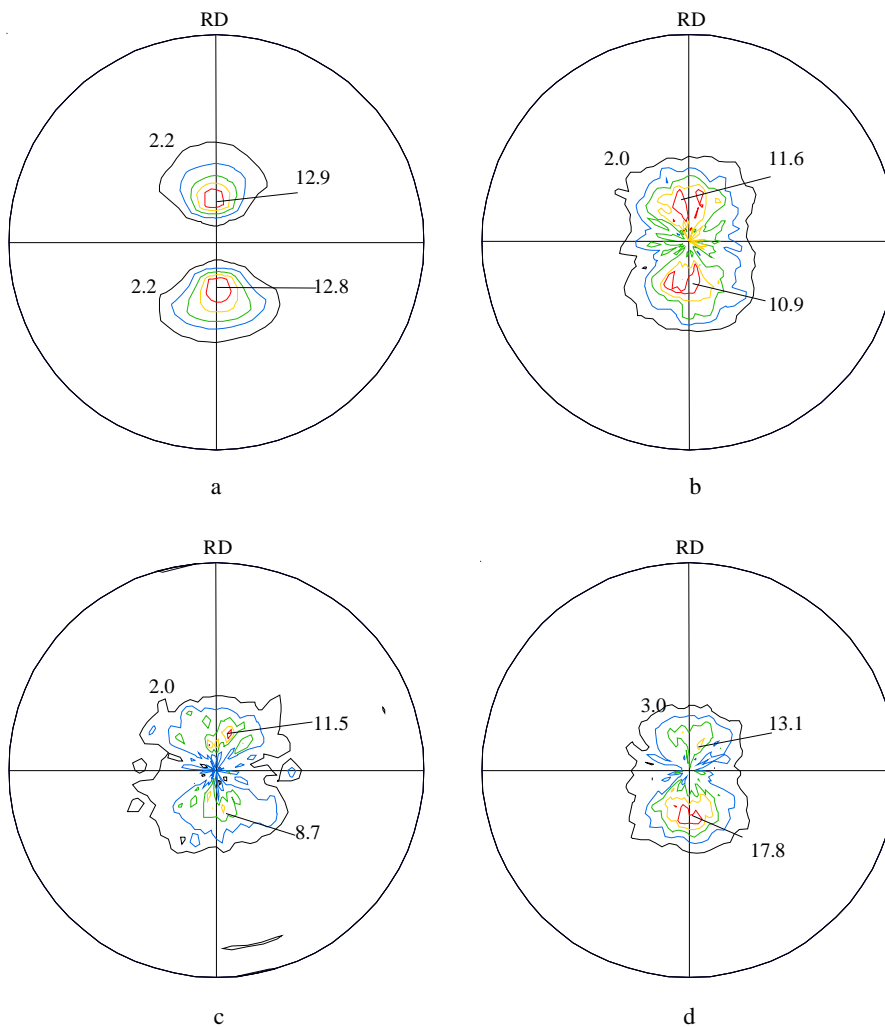
annealing of samples oriented parallel to the field intensifies processes occurring during annealing without field and results in stronger decrease of the intensity of texture components as well as in increase of the difference between their intensities. At present there is only one known effect of magnetic field on structural changes of diamagnetic materials

Figure 6. Calculated pole figures of Zn-1.1%Al sheet samples. (a) after rolling; (b) after annealing without field; (c) and (d) after annealing under the field, (c) samples orientated along to the field; (d) samples tilted at 20° to the field about the TD.

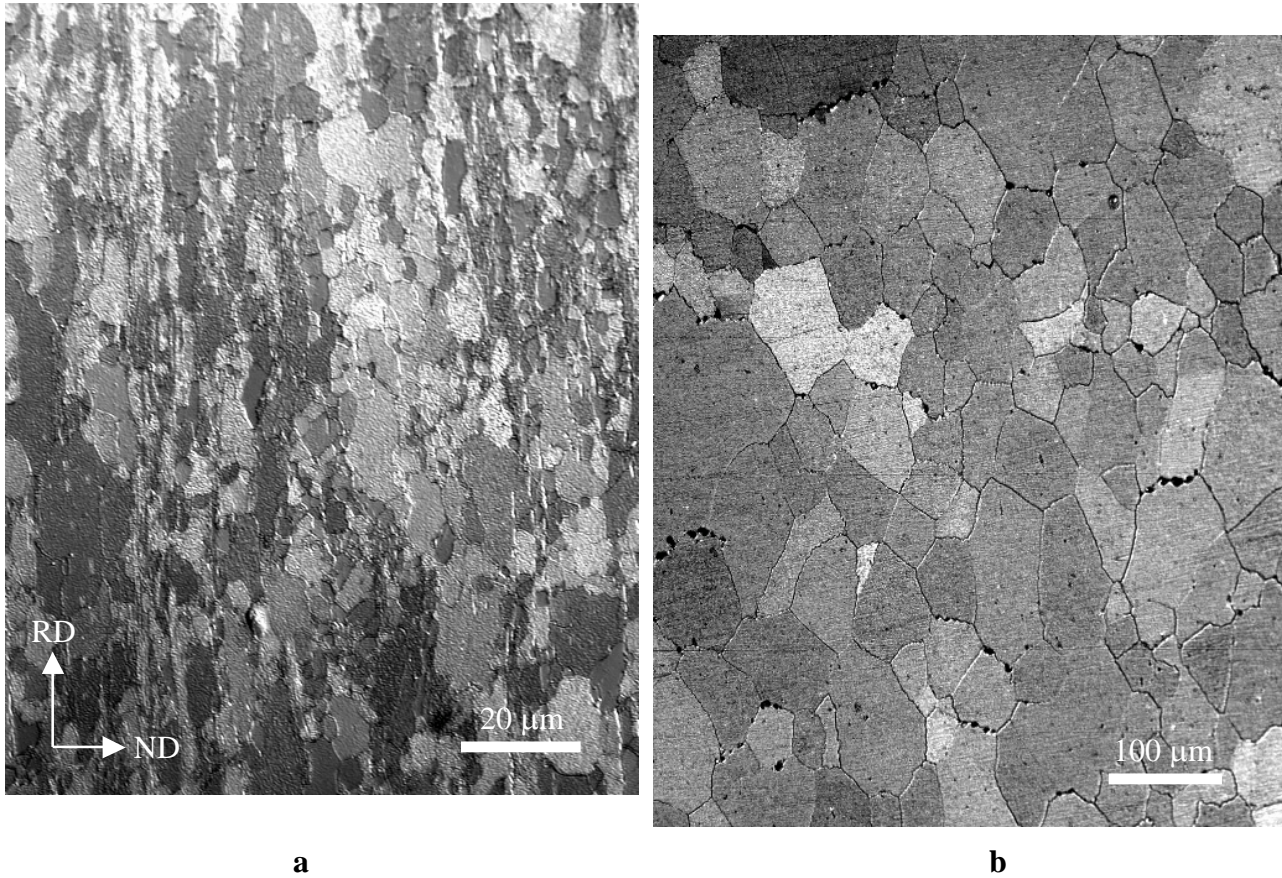a   b

Figure 7. Micrographs of Zn-1.1%Al sheet: (a) After rolling and (b) after magnetic annealing. [1, 2].

At room temperature Zn has the following magnetic susceptibilities: $\chi_{\parallel} = -0.190 \cdot 10^{-6}$ and $\chi_{\perp} = -0.145 \cdot 10^{-6}$ [3], where $\chi_{\parallel}$ and $\chi_{\perp}$ magnetic susceptibilies parallel and perpendicular to hexagonal (or c or <0001>) axes, respectively. The maximum driving force for boundary migration in Zn in the case of magnetic field of H=32 T and difference in magnetic susceptibilies of $\Delta\chi = \chi_{\perp} - \chi_{\parallel} = 0.45 \cdot 10^{-7}$ is p_{max}=230 J/m^3. For comparison, this driving force for boundary migration is half of that in polycrystalline bismuth at 8 T magnet field inductivity [1]

and about eight times higher than that in Bi bicrystals [2]. In Zn, however, this force can appear in the case of specific boundary misorientation of 90° and c-axes oriented parallel and perpendicular to the field. For other bicrystals this force should be lower. Therefore, in a polycrystalline material structural changes depend on type of crystallographic texture and boundary misorientation distribution. In general, these two parameters cannot be viewed as independent. It is reasonable to expect that grains related to different components should have the highest proportion of common boundaries with misorientations within the range of 30-40°. Figure 8 illustrates the statistical distributions of boundary misorientations obtained for two Zn-0.16%Cu-0.076%Ti sheet alloys with and without grain refiner [4]. They have the same two-component pole figure as in the case of Zn-1.1%Al sheet. Interestingly, for both compositions there is no expected relationship between texture and boundary misorientation distribution. The boundaries with misorientions within 30-40° have even lower frequency than others. Therefore, the grains that belong to one texture component cannot grow in the expense of grains that belong to the other one. That is why there is no simultaneous increase of the one texture component and the decrease of the other one during annealing of Zn-1.1%Al sheet. For samples oriented parallel to the field, c-axes of grains related to the texture components are tilted at ~73° to the field. Consequently, their free energy does not reach a minimum value. The decrease in the intensity of texture components can be a result of the growth of grains with c-axes perpendicular to the field in the expense of the grains corresponded to those components. When basal planes become parallel to the field the magnetic free energy of the respective grains becomes minimum, due to the minimum value of magnetic susceptibility. The difference of the magnetic free energy in differently oriented grains exerts a driving force for the growth of grains having basal planes parallel to the field. Due to this additional driving force these grains grow faster than others and result in the increase of one of the texture peaks. At the same time the intensity of other texture component do not decrease despite the fact that magnetic susceptibility of related grains becomes even higher than in the case of the sample oriented parallel to the field. This result may indicate that fast growing grains change the environment of the grains with high magnetic susceptibility and/or neighboring grains being reoriented also achieve high susceptibility so the magnetic driving force decreases significantly.
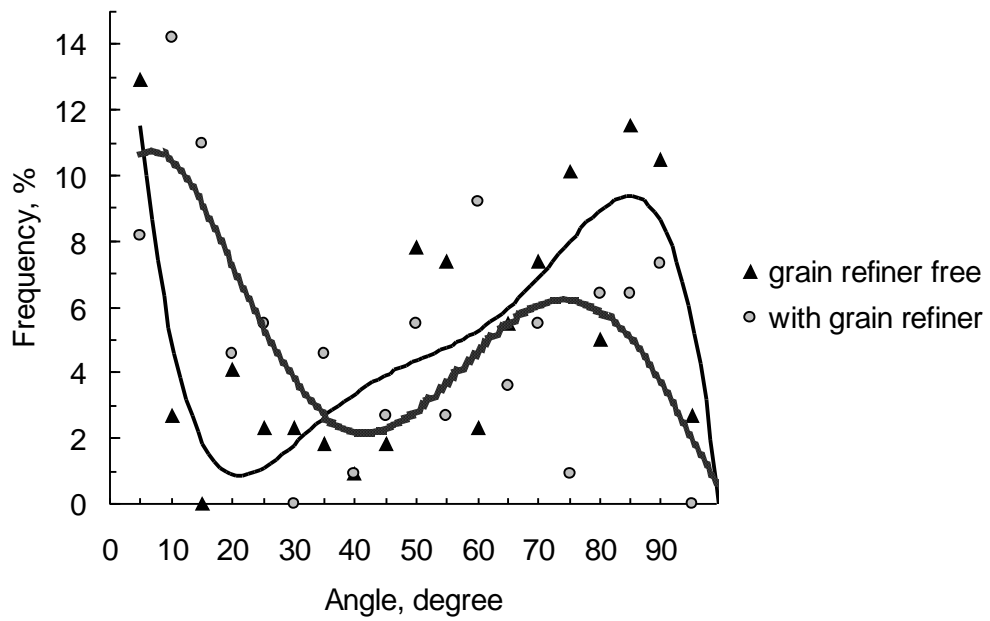
Figure 8. Grain boundary distribution by angles of misorientation in Zn-0.16%Cu-0.076%Ti alloy with and without grain refinement [4].

2.2. Magnetic Annealing of $Nd_2Fe_{14}B/\alpha$-Fe-type Nanocomposites

In this study, crystallographic textures, enhanced exchange coupling and in-plane magnetic anisotropy in magnetically annealed $Nd_{2.4}Pr_{5.6}Dy_1Fe_{84}Mo_1B_6$ nanocomposites have been studied. Compared with the sample annealed without a magnetic field, the magnetic annealing results in a noticeable improvement of the (110) texture of α-Fe perpendicular to the ribbon plane and in-plane uniaxial magnetic anisotropy (Figure 9). In the mean time, there was a noticeable improvement in the coercivity $_iH_c$, the remanence $4\pi M_r$, and energy product $(BH)_{max}$ for magnetic annealed $Nd_{2.4}Pr_{5.6}Dy_1Fe_{84}Mo_1B_6$ alloys. Especially, $(BH)_{max}$ at 50 K was enhanced by 43.7 % after magnetic annealing in a 19 T field. The kink at the demagnetization curve disappeared and, in addition, a much better squareness of the demagnetization curves was observed after the magnetic annealing (Figure 10). The improvement in the hard magnetic properties after magnetic annealing is a comprehensive result of the crystallographic textures, magnetic-field-induced enhanced in-plane uniaxial magnetic anisotropy, and an enhanced exchange coupling due to optimizations of the nanostructure by magnetic annealing.
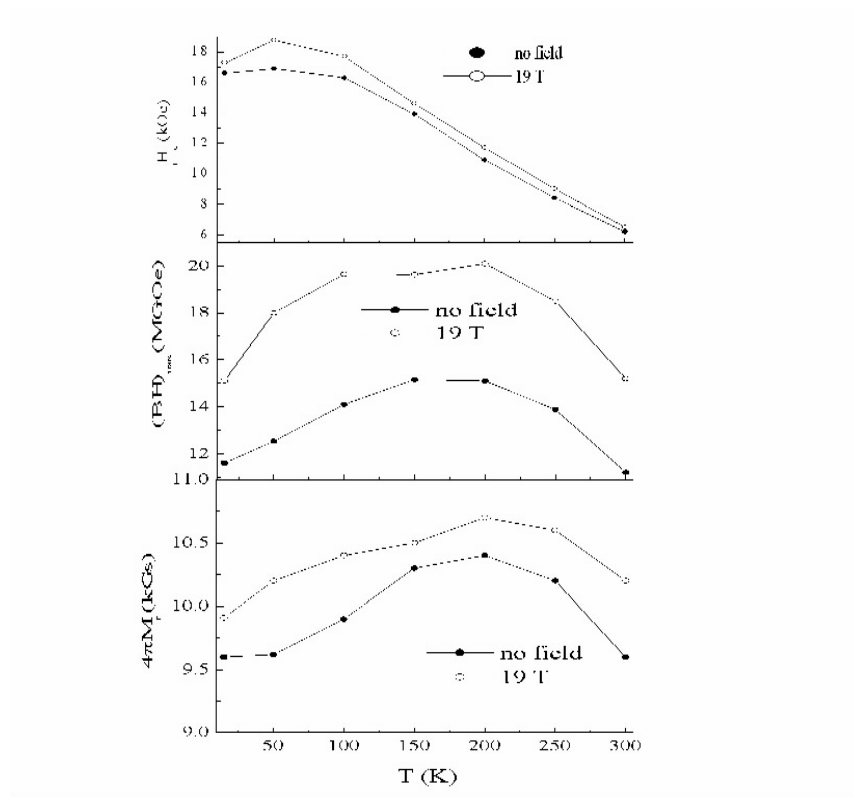
Fig.9. Dependence of $_iH_c$, $(BH)_{max}$ and $4\pi M_r$ on temperatures for $Nd_{2.4}Pr_{5.6}Dy_1Fe_{84}Mo_1B_6$ ribbons annealed at 690°C for 20 min without and with a 19 T in-plane field..
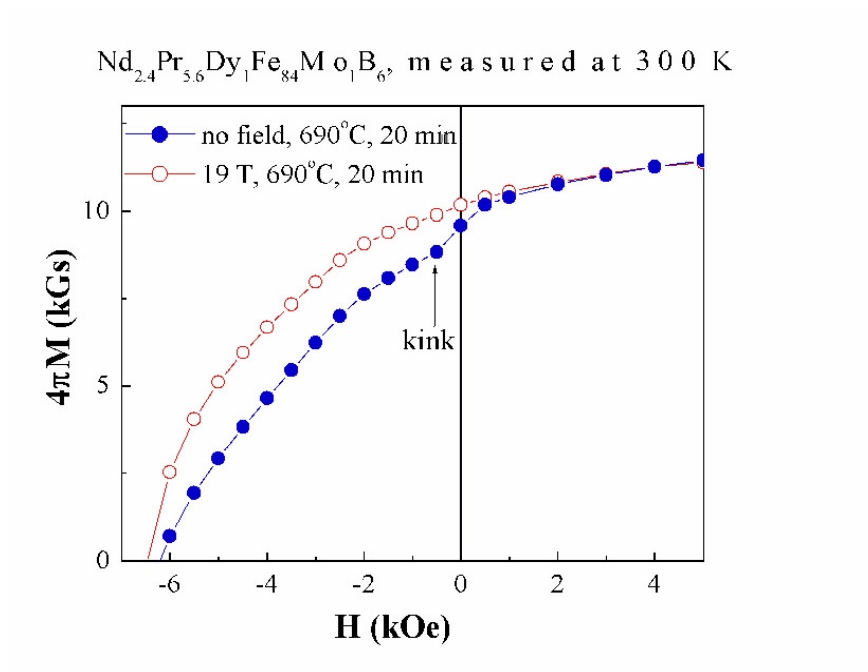

Fig.10. Low field portion of half hysteresis loops of the melt-spun $Nd_{2.4}Pr_{5.6}Dy_1Fe_{84}Mo_1B_6$ ribbons annealed at 690°C for 20 min without and with a 19 T in-plane field.

2.3. Texture and magnetic properties of FePd improved by magnetic annealing

High magnetic field annealing was applied to FePd alloy to improve the preferred orientation distribution (texture) and obtain the desirable magnetic anisotropy. A rigorous texture characterization method was used to analyze the crystal orientation distribution of the annealed FePd. As compared with annealing without magnetic field, the high magnetic field annealing increases the volume fraction of crystal grains with c-axes aligned along the annealing magnetic field direction. A uniaxial magnetic anisotropy was also observed in the magnetic annealed FePd alloy. It is very important to control the microstructure of the magnetic materials because textured or anisotropic magnetic materials usually show better performance in device applications. Among many methods to achieve the desirable texture and magnetic properties, magnetic field processing is a popular one. For magnetically soft materials, it is well known that a well-defined uniaxial anisotropy can be obtained due to the atomic pair anisotropy induced by the magnetic field annealing. For permanent magnetic materials, the loose powders of single crystal grains can rotate so as to align their easy magnetization axes along with the magnetic field direction. Further sintering the aligned grains will obtain the anisotropic permanent magnets. It is also worthy to mention that the oriented permanent magnets can be obtained by solidification from the molten status in a high magnetic field [5].

However, up to date, only a few high magnetic field annealing experiments (in the magnetic field of several Tesla) have been done on magnetic materials, and the mechanisms through which the high magnetic annealing field plays a role on microstructures and magnetic properties are still unclear [7-11]. It was found that annealing the cold-rolled Fe-Si sheet [7] in a high magnetic field of 10T parallel to the rolling direction enhanced the selectivity of the <001> axis alignment. High magnetic field (1.5T) annealing in another system, Armco iron, was also studied [8]. The grains with <100> parallel to the external field would nucleate preferentially. High magnetic field annealing was also applied in FePd system by Tanaka et. al. [9]. It was

claimed that a so-called mono variant $L1_0$ structure was obtained by high magnetic field annealing at 780K under 10T. However, the crystal orientation analysis method used in their experiments was rough and incomplete, and there was no study in magnetic anisotropy. In our previous study on ferromagnetically soft FeSi alloy [10] and diamagnetic ZnAl alloy [10], it was found that the preferred orientation was improved by the high magnetic field annealing. No corresponding magnetic properties were reported either in early studies.

The equilibrium phase diagram of the FePd system shows five distinguishable regions at low temperature as a function of the atomic content of Pd [12]. The equiatomic FePd undergoes an order-disorder transition at about 923K from a disordered fcc to an ordered $L1_0$ tetragonal structure. In tetragonal FePd, the c-direction is an easy magnetization axis. In this letter, the effects of the high magnetic field annealing on the phase transition of FePd alloy and the orientation distribution of the crystals in FePd $L1_0$ phase were studied. Here a robust crystal orientation distribution study method was used to understand the microstructure and vibrating sample magnetometry (VSM) to characterize the corresponding magnetic properties.

The alloy ingot of the FePd was prepared by arcmelting of Fe and Pd in an argon atmosphere. FePd samples sealed in a vacuum tube of the quartz glass were annealed in a 30T magnetic field for 6 hours at 650°C. The magnetic field direction (H_A) during annealing is in the plane of the FePd sheet along the sample's longitudinal direction. As a comparison, the same as-prepared FePd samples are annealed in a similar process except the exposure in the magnetic field. Texture was measured using a Philips X'Pert PW3040 MRD X-ray diffractometer, equipped with a pole figure goniometer, operating at 40kV and 45mA and employing Ni filtered Cu Kα radiation, as described before [13]. Incomplete pole figures of

FePd (002), (111), (113), (200), (202) were obtained from measurements. After correcting the geometric defocusing and background X-ray intensity, harmonic algorithm implemented in PopLA was used to calculate the crystal orientation distribution function from which the complete recalculated pole figures were constructed. Furthermore, magnetic properties were measured by VSM.

X-ray diffraction indicates that magnetic annealing has obvious effects on the texture of the FePd alloy, as shown in Fig.1. It is clear that the high magnetic field annealing enhances the phase separation between α-Fe phase (Fe (110)) and FePd alloy phases (FePd (111) and (002) etc.). Moreover, the high magnetic field annealing enhances the relative intensity of FePd (002) peak to that of FePd (111) peak.
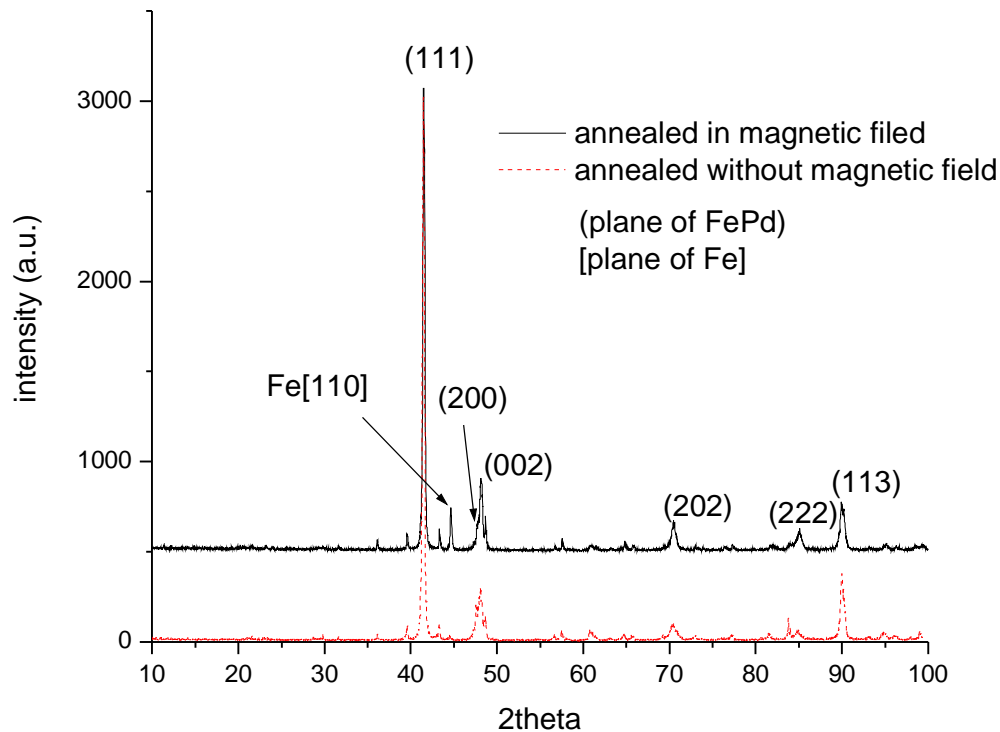

Fig.11. X-ray diffraction patterns of FePd samples annealed without a magnetic field and in a magnetic field.

Fig.12 illustrates (002) pole figures of annealed FePd samples. MD is the longitudinal direction of the sample (the direction of the annealing magnetic field H_A); TD the transverse direction, while the crosshair corresponds to the normal direction of the sample. In magnetic annealed samples the distribution density of crystals with c-axis parallel to the H_A (Fig. 12a) is 2.05 times random density. This means that the high magnetic field annealing tends to align the c-axis along the direction of the annealing field. In samples annealed without magnetic field (Fig. 12b) the density of crystals with c axis along the longitudinal direction is only 1.21 times random density. This means that the FePd annealed without field has no trend to show uniaxial crystal anisotropy.

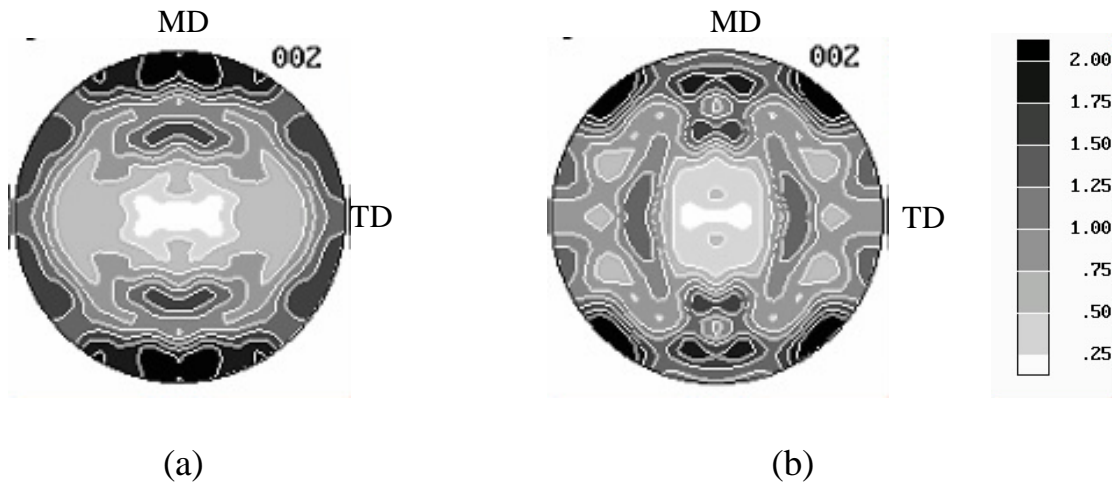(a)   (b)

Fig. 12. (002) pole figures of FePd annealed (a) in a magnetic field and (b) without magnetic field

Texture analysis indicates that annealing under high magnetic field does improve the orientation distribution of crystals in the FePd samples, although far from the mono-variant structure. Since more crystal grains have their easy magnetization axis parallel to the annealing field direction as compared with those annealed without magnetic field, the uniaxial anisotropy is expected for the magnetic annealed FePd samples. Fig.13 shows the hysteresis loops of FePd

samples of different processes, i.e., annealed without field, and annealed with field. The samples used in VSM measurements were circular sheet of the same dimensions. The magnetic field used in VSM measurements was in the plane of the sheet, such as along MD and TD directions in the plane. In this case, the demagnetization factor is the same for all the hysteresis loops when the external field is applied in the plane of the circular sheet. Therefore, any differences in the hysteresis loops, if exist, originates from the intrinsic anisotropy. For the magnetic annealed samples, the differences (such as difference in saturation fields) in hysteresis loops of MD and TD configurations clearly show magnetic anisotropy which can be attributed to the alignment of the grains. According to the X-ray results in Fig.12 (a), the easy magnetization axis of the grains annealed in the high field has a larger possibility to align along the MD. Therefore, a smaller saturation field was found in MD direction than that in TD direction. By contrast, in non-magnetic annealed samples there is no detectable difference in the hysteresis loops between MD and TD in the plane of the sheet sample. Only one hysteresis loop for this annealed sample was shown in Fig.3. This is in agreement with the pole figure in Fig.2 (b), where the distribution of easy magnetization axis is far from the uniaxial anisotropy.
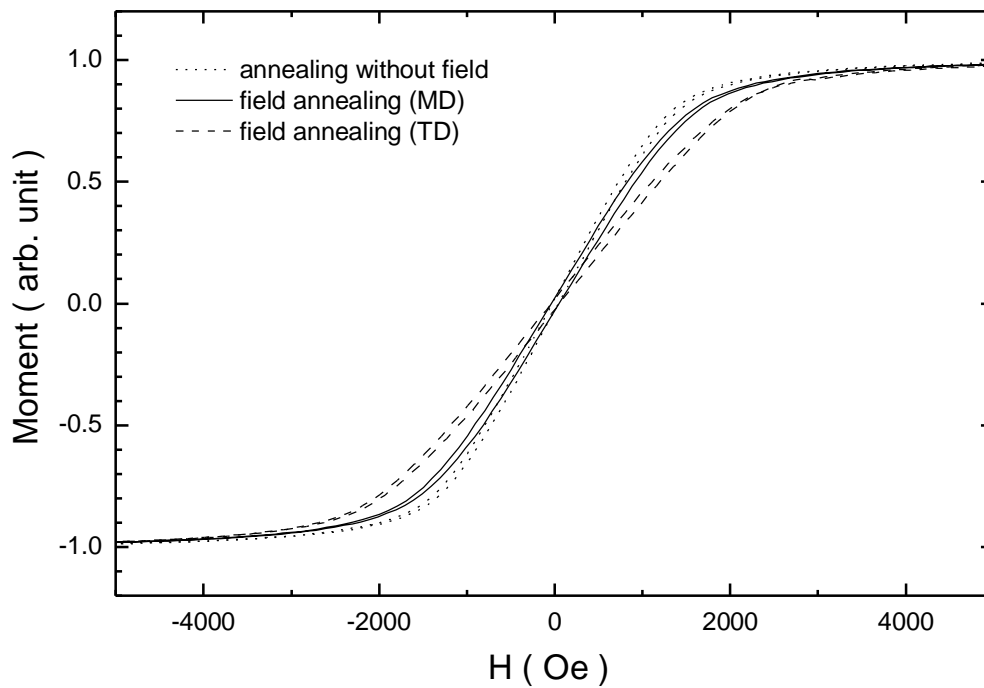
Fig.13. The hysteresis loops of the FePd samples annealed in the magnetic field and annealed without magnetic field.

It is worthy to mention that the alignment of the grains and the magnetic anisotropy may be further enhanced if the FePd samples were annealed in the high magnetic field for longer time. According to the nonmagnetic annealing process under the same annealing conditions, the equilibrium phases may be reached after about 100 hour annealing. Although the FePd samples were only annealed for 6 hours in the present experiments, significant magnetic field effects have been found in two independent experiments (X-ray and VSM measurements). From the viewpoint of the free energy of the FePd system, different FePd phases and grains of magnetic crystal anisotropy may have different energy in the high magnetic field for different directions if the magnetic crystal anisotropy energy and the magnetostriction energy were taken into account. Therefore, when the FePd alloy was annealed in a high magnetic field, the FePd system may gradually evolve into different phases and show anisotropic nucleation and growth as compared with the case of the nonmagnetic annealing. However, quantitative analysis on the high magnetic field annealing mechanisms still need further research work.

In conclusions, the high magnetic field annealing can enhance the phase separation of the disorder uniform FePd alloy, and induce the microstructural and magnetic anisotropy. Since FePd system has a potential to be a candidate for the recording media and the magnetic anisotropy is highly desirable in many applications, the magnetic field induced structural and magnetic anisotropy may have great contribution to technology development.

Summary

In summary it has been shown that magnetic field can affect texturing of materials by either of two mechanisms. These two mechanisms have been identified as grain boundary motion and solidification from the melt. In the case of Zn, FePd and Fe-Si and Terfenol-D, and the nano-

magnets the dominating mechanism is identified as grain boundary motion and in the case of NdFeB solidification from the melt appears to be the dominating mechanism. Depending on the orientation of the specimen with respect to the applied field texture components could be strengthened or weakened.

A number of Journal papers and Proceedings have been published as a result of this funding:

1. A.D. Sheikh-Ali and H. Garmestani, Assessment of Contribution of Intragranular Slip to Grain Boundary Sliding in Bicrystals, Materials Science Forum (to be published).A.D. Sheikh-Ali, J.A. Szpunar and H. Garmestani, Stimulation and Suppression of Grain Boundary Sliding by Intragranular Slip in Zinc Bicrystals, Interface Science.- 2003, v.11, pp. 439-450.
2. A.D. Sheikh-Ali, J.A. Szpunar and H.Garmestani, Grain Boundary Sliding during Creep: Role of Boundary Misorientation and Strain Compatibility, Minerals, Metals and Materials Society/AIME, Creep Deformation: Fundamentals and Applications, pp. 127-136, 2002.
3. A. D. Sheikh-Ali; H. Garmestani, "On the independent behavior of grain boundary sliding and intragranular slip during superplasticity", Trans Tech Publications, Materials Science Forum, vol. 357-359, pp. 393-398, 2001.
4. H. Garmestani, S. Lin, B. Adams, S. Ahzi, "Statistical Continuum Theory for Texture Evolution of Polycrystals", Journal of the Mechanics and physics of Solids 49, (2001) 589-607.
5. A.D. Sheikh-Ali and H. Garmestani, Evolution of Surface and Bulk Textures during Superplastic Deformation in a Zn-1.1%wt. Al alloy, Scripta Materialia (submitted).
6. H. Garmestani, A.D. Sheikh-Ali, The Effect of Crystallographic Texture on Grain Boundary Sliding during Superplastic Deformation in Zn-1.1%wt. Al Alloy, Scripta Materialia (submitted).
7. A.D. Sheikh-Ali, D.A Molodov and H. Garmestani, *Texture Development in Zn-1.1%Al under Strong Magnetic Field,* Trans Tech Publications, Materials Science Forum Vols. 408-412 (2002) pp. 961-966.
8. C. Bacaltchuk, Ebrahimi M, Branco, G., H. Garmestani, A.D. Rollett "Effect of Magnetic Field Applied During Secondary Annealing on Texture and Grain size of Silicon Steel". Scripta Materialia, vol 48, 1343-1347, (2003).
9. D.S. Li, H. Garmestani, Scott Schoenfeld, "Evolution of Crystal Orientation Distribution Coefficients During Plastic Deformation", *Scripta Materialia, Volume 49, Issue 9, November 2003, 867-872.*

3.0 Personnel and students:

Dr. Askar Sheik-Ali together with Dr. Lamar Meda served as the post-doctoral research associates working on this project on 1/3 time (Meda) and (1/2) time (Sheik-Ali). Dr. Marwan Haik and Dr. Klaus Dahmen served as research associates at different periods of time. Two graduate students, Cristiane Bastos Bacaltchuk and Saleh Al-Haik (both Ph.D.), worked with Dr. Garmestani and the Post-docs. Antoine Berret (African) is another graduate students who also worked on the proposal both as an undergraduate student and a graduate student. Gail Jefferson (Female and African American) and jamaa bouhattate Reeshema Burrell (Female and African American) were two other graduate students are are presently involved in the various aspects of the project. Ph.D. student Dongsheng Li worked on the project (effect of magnetic field on polymer materials) together with Dr. Shishen Yan who worked on a joint project (nano-magnetics, Met-Materials) with Dr. Liu at Texas University.

References

1.   Mullins W.W., *Acta Metall.,* **4,** 421-432 (1956).
2.   Molodov D.A., Gottstein G., Heringhaus F. and Shvindlerman L.S., *Acta Mater.,* **46,** 5627-5632 (1998).
3.   Mac Clure J. W., Marcus J. A., *Phys. Rev.,* **84,** 787-788 (1951).
4.   Philippe M.J., Beaujean I., Bouzy E., Diot M., Wegria J. and Esling C., *10th International Conference on Textures of Materials, Clausthal, Germany, 20-24 Sept. 1993 (ICOTOM-10)*, Mater. Sci. Forum, **157-162,** 1671-1680 (1994).
5.   B. A. Legrand, D. Chateigner, R. Perrier de la Bathie, and R. Tournier, J. Magn. Magn. Mater. **173**, 20 (1997).
6.   N. Masahashi, M. Matsuo, and K. Watanabe, J. Mater. Res. **13**, 457 (1998).
7.   H. O. Martikainen, and V. K. Lindroos, Scand. J. Metal. **10**, 3 (1981).
8.   K. Tanaka, T. Ichitsubo, and M. Koiwa, Mater. Sci. Eng. **A312**, 118 (2001).
9.   C. M. B. Bacaltchuk, G. A. Castello-Branco, M. Ebrahimi, H. Garmestani, and A. D. Rollett, Scripta Mater. **48**, 1343 (2003).
10.   A.D. Sheikh-Ali, D.A. Molodov, and H. Garmestani, Scripta Mater. **46**, 857 (2002).

11. J. I. Pérez-Landazábal, C. Gómez-polo, V. Recarte, J. Vergara, R.J.Ortega, and V.Madurga, J. Magn. Magn. Mater. **196-197**, 179 (1999).

12. D. Li, H. Garmestani, S.R. Kalidindi, and R. Alamo, Polymer **42**, 4903 (2001).